Supplementary information for

Ordered growth of $Cs_2AgBiBr_6$ double perovskite on PEIE-decorated SnO_2 for efficient planar solar cells

Wanjiang Wang[a], Linsong Hou[a], Haihua Hu[b], Binbin Chang[a], Yuqi Yuan[a], Ping Lin[a], Peng Wang[a], Xiaoping Wu[a], Xuegong Yu[c], Lingbo Xu[a, *], and Can Cui[a, *]

[a] Key Laboratory of Optical Field Manipulation of Zhejiang Province, Department of Physics, School of Science, Zhejiang Sci-Tech University, Hangzhou 310018, People's Republic of China

[b] Hangzhou City University, Hangzhou 310015, China

[c] State Key Laboratory of Silicon Materials, School of Materials Science and Engineering, Zhejiang University, Hangzhou 310027, People's Republic of China

[*] Corresponding author. Email: xlb@zstu.edu.cn (L. Xu), cancui@zstu.edu.cn (C. Cui)

1 Experimental Section

1.1 Materials

Polyethylenimine, 80% ethoxylated solution (PEIE, 37 wt.% in water, average Mw~110000), 2-propanol (IPA, ≥99.5%), 4-tertbutylpyridine (4-TBP, ≥96%), acetonitrile (ACN, ≥99.8%) and dimethyl sulfoxide (DMSO, 99.9%) were purchased from Sigma-Aldrich. SnO_2 (colloidal dispersion, 15 % in H_2O), AgBr (99.5 %) and $BiBr_3$ (99%) was obtained from Alfa Aesar.2,2′,7,7′-Tetr akisn [N, N-di(4-methoxyphenyl) amino] −9,9′-spirobifluorene (Spiro-OMeTAD, ≥99.5%), LiTFSI (≥99.0%) and Co(III)TFSI (≥99.0%) and CsBr (99.9%) were purchased from Xi'an Polymer Light Technology Corporation. Chlorobenzene (CB, ≥99.5%), MoO_3

(≥99.9%), and hydrobromic acid (HBr, 48 wt. % in water) were purchased from Aladdin.

1.2 Preparation of $Cs_2AgBiBr_6$ powders

Slight modifications were made according to the reported synthesis.[1] First, 852 mg of CsBr, 898 mg of $BiBr_3$, and 376 mg of AgBr were dissolved in 20 ml of HBr. The solution was stirred at 110 °C for 2 h and then cooled naturally to room temperature. The solution was poured out and the orange powder was removed and washed 3-5 times with ethanol. Finally, the powder was moved to a vacuum drying oven and dried at 70 °C overnight to obtain $Cs_2AgBiBr_6$ crystal powder.

1.3 Preparation of $Cs_2AgBiBr_6$ films

531 mg (0.5 mmol) of $Cs_2AgBiBr_6$ powder was dissolved in 1 ml DMSO to formulate a 0.5 M precursor solution. The precursor must be stirred at 80 °C for over 3 h to ensure complete powder dissolution. The PEIE is diluted to different concentrations and named PEIE-x. For example, PEIE-0.2 means that the concentration of PEIE in solution is 0.2 mg/ml. The substrate was treated with ultraviolet-O_3 for 20 min before spin coating. The PEIE-x solution was spin-coated on the substrate at 4000 rpm for 30 s, then annealed at 100℃ for 10min. Following ultraviolet-O_3 treatment for 15 min, they were transferred to an N_2 glove box to prepare $Cs_2AgBiBr_6$ films. The substrate and $Cs_2AgBiBr_6$ precursor were preheated on a heating table at 80 °C for more than 10 min. The $Cs_2AgBiBr_6$ precursor was spin-coated on the substrate at 2000 rpm for 60 s, and 250 μl IPA was added dropwise as an anti-solvent 20 s before the end of the spin-coating process. After the spin coating, the thin films were annealed at 250 ℃ for 5

min.

1.4 Fabrication of solar cell devices

This work adopts the n-i-p planar solar cell structure based on SnO_2 as the electron transport layer. Firstly, the etched ITO glass was cleaned by ultrasonic cleaning with deionized water, ethanol, acetone, and isopropanol in sequence for 20 min, and treated with ultraviolet-O_3 for 20 min. Next, the SnO_2 precursor solution (The SnO_2 stock solution was dissolved with deionized water at a volume ratio of 1:4 and stirred at room temperature for 6 h to obtain the SnO_2 precursor) was spin-coated on ITO at 3000 rpm for 30 s, followed by annealing at 150 ℃ for 30 min. Then, the $Cs_2AgBiBr_6$ absorber layer was prepared following procedure **1.3** after the films were treated with ultraviolet-O_3 for 20 min. Next, Spiro-OMeTAD solution was spin-coated onto the $Cs_2AgBiBr_6$ film at 3000 rpm for 35 s. For Spiro-OMeTAD solution, the Spiro-OMeTAD (72.25 mg) was dissolved in 1 mL of chlorobenzene,18.5 μl of TBP and 17.5 μl of 520 mg/mL Li-TFSI. Finally, 10 nm of MoO_3 and 100 nm of silver electrode were vaporized on the hole transport layer at 10^{-3} Pa. The effective area of the device was controlled to 0.1 cm^2 by a mask plate.

1.5 Characterizations

Scanning electron microscope (SEM) images were taken on a Hitachi S4800 (Japan) using a 3 kV accelerating voltage. X-ray diffraction (XRD) patterns of perovskite films were examined by a Bruker D8 Advance diffractometer with Cu Kα radiation (λ = 0.154056 nm). The spectrophotometer measured the ultraviolet-visible (UV–vis) absorption spectra (UV-2600, Shimadzu). The steady-state

photoluminescence (PL) and time-resolved photoluminescence (TRPL) data were measured by the PL spectrometer (Fluotime300, PicoQuant). The excitation wavelength of PL and TRPL measurements is 375 nm. Raman spectra of $Cs_2AgBiBr_6$ films were recorded by laser confocal microraman spectrometer; a diode-pumped solid-state laser with a wavelength of 532.0 nm was used as a source of excitation. The ultraviolet photoelectron spectroscopy (UPS) measurements were performed on an Axis supra (Kratos, Shimadzu). The photoelectrons from UPS were counted with a hemispherical analyzer with an overall resolution of 0.05 eV, as determined from the width of the Fermi step measured on a gold substrate cleaned by Ar-ion sputtering. All the UPS measurements of the onset of photoemission for determining the work function were done using standard procedures with a − 9.8 V bias applied to the sample. The current density-voltage (J-V) curves were measured by a Keithley 2400 source meter under the illumination of AM 1.5 G (100 mW/cm^2) provided by a solar simulator (Zolix, SolarIV-1000A). The external quantum efficiency (EQE) was measured in the wavelength range of 300-850 nm, using an EQE measurement system (Model QEX10, PV Measurements). Electrochemical impedance spectroscopy (EIS) was measured by an electrochemical workstation (VersaSTAT 4, Princeton Applied Research) in the dark with a frequency ranging from 1 Hz to 1 MHz.

2 Figures

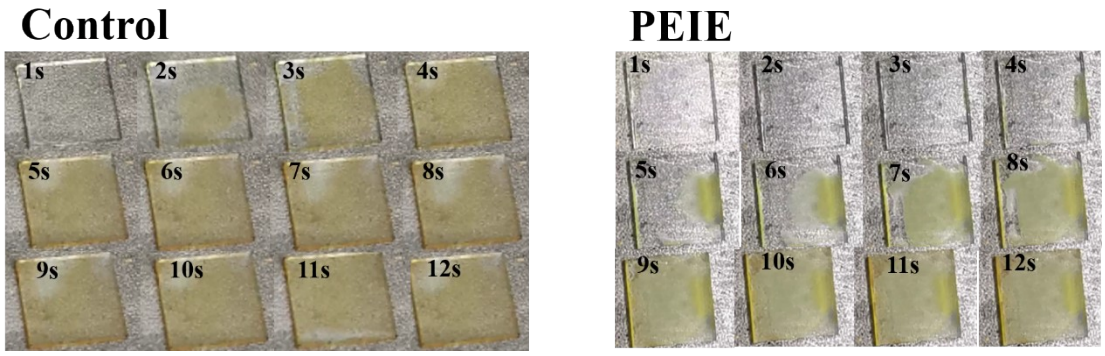

Fig. S1. Color conversions of $Cs_2AgBiBr_6$ films on different substrates during thermal treatment.

Each image is taken at an interval of 1 second.

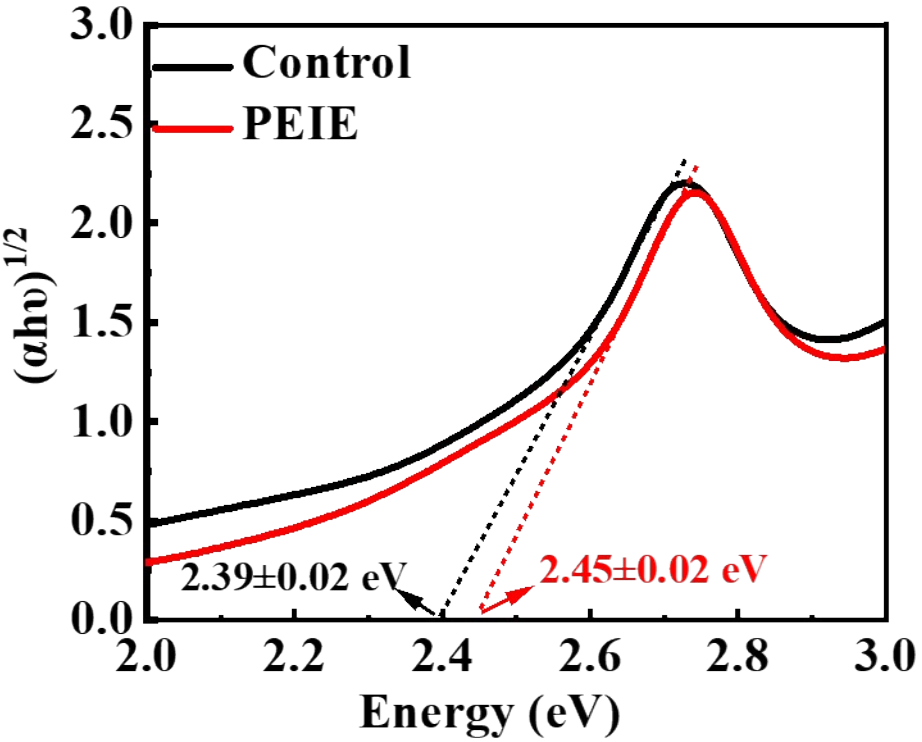

Fig. S2. Tauc plots of $Cs_2AgBiBr_6$ films on different substrates.

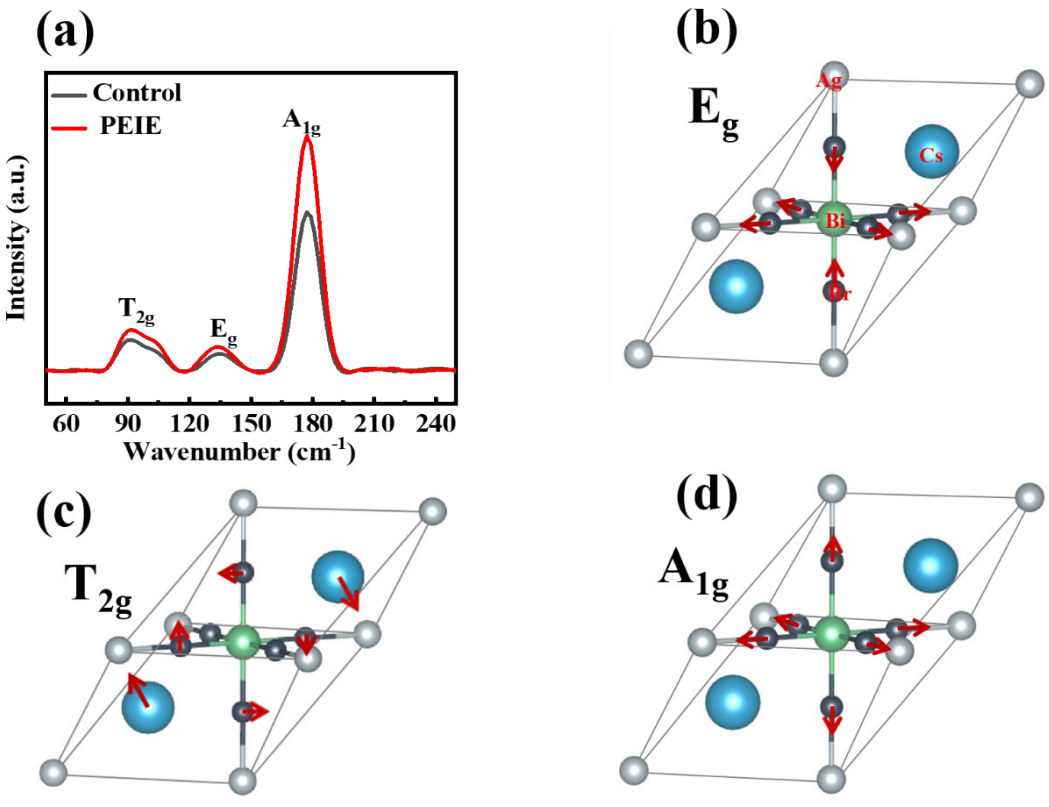

Fig. S3. (a) Raman spectra of $Cs_2AgBiBr_6$ films on different substrates. The Raman spectra of $Cs_2AgBiBr_6$ consist three peaks at 74 cm^{-1}, 139 cm^{-1}, and 180 cm^{-1}, which correspond to T_{2g} mode, E_g mode, and A_{1g} mode, respectively[2, 3]. The schematic diagrams of these modes are shown in **Fig. S3 (b-d)**. The E_g mode is due to the asymmetric stretching around the Bi atom. The T_{2g} mode is related to the shear motion of Cs atoms around the Br. The A_{1g} longitudinal optical (LO) phonon mode is related to the symmetric stretching vibration of the Bi atoms around the Br atom in the octahedron.

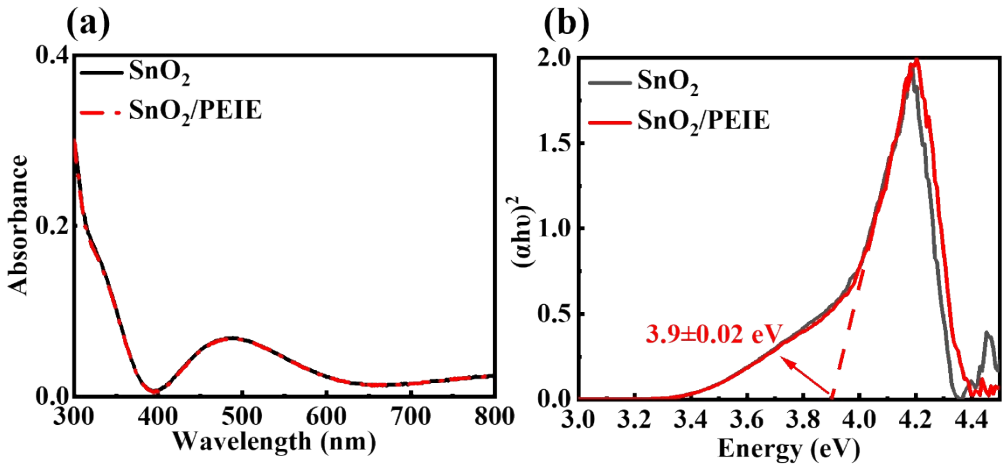

Fig. S4. (a) UV-vis absorption spectra of SnO_2 and SnO_2/PEIE films. (b) Tauc plots of SnO_2 and SnO_2/PEIE films.

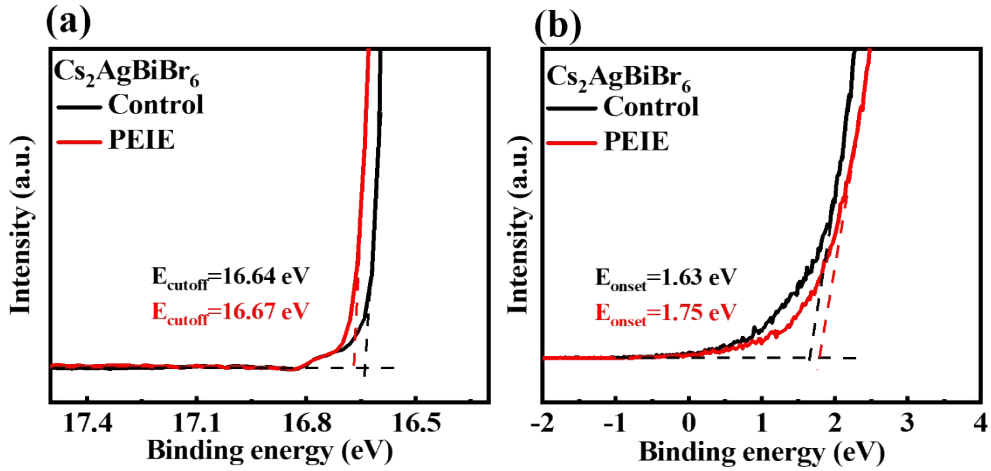

Fig. S5. Secondary electron cutoff regions (a) and onset regions (b) of UPS spectra for $Cs_2AgBiBr_6$ films on different substrates.

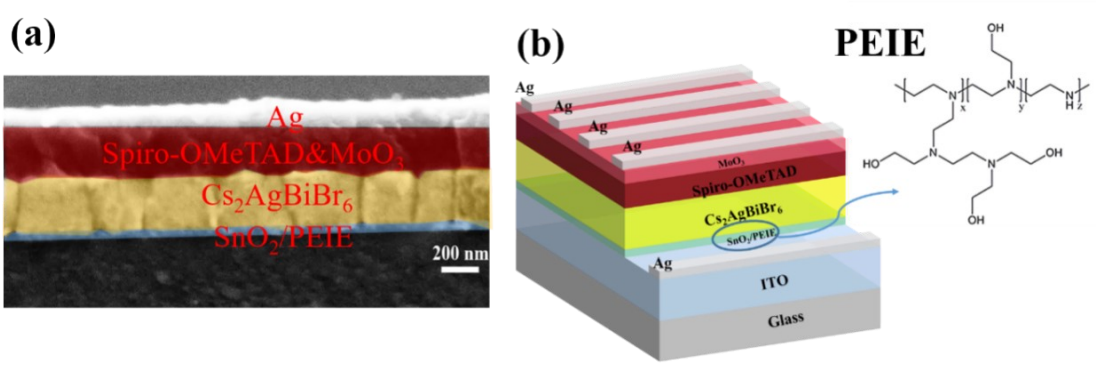

Fig. S6. (a) The cross-sectional SEM and (b) schematic structure of $Cs_2AgBiBr_6$ PSCs.

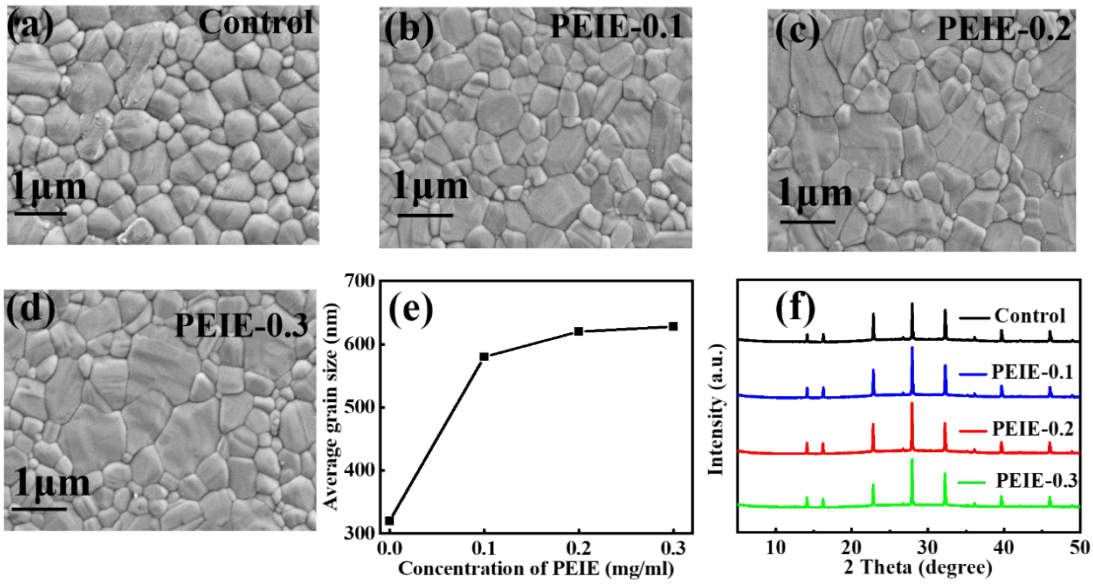

Fig. S7. (a-d) Top-view SEM images of $Cs_2AgBiBr_6$ films deposited on substrates with different PEIE concentrations. (e) Average grain size of $Cs_2AgBiBr_6$ films on different substrates. (f) XRD patterns of $Cs_2AgBiBr_6$ films on different substrates.

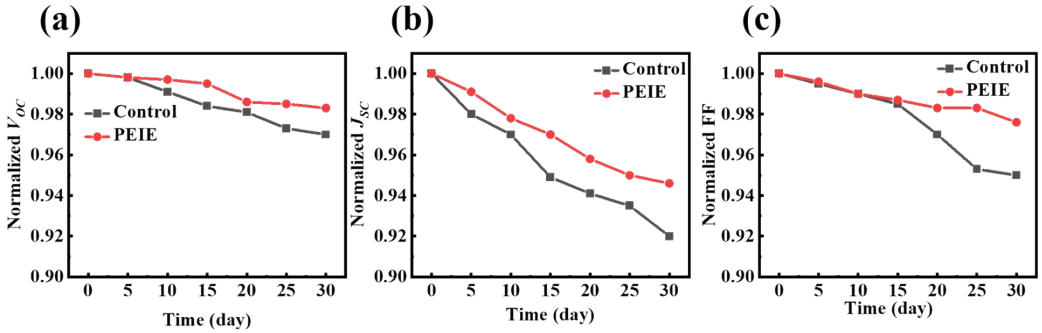

Fig. S8. Long-term stability test of (a) *Voc*, (b) *Jsc*, and (c) FF (temperature:20~30 °C, 20~30 % relative humidity).

3 Tables

Table S1. Fitting parameters for TRPL measurements of $Cs_2AgBiBr_6$ films deposited on different substrates.

Sample	τ (ns)	β	$<\tau>$ (ns)
Glass/$Cs_2AgBiBr_6$	4.21	0.40	13.51
SnO_2/$Cs_2AgBiBr_6$	1.88	0.49	3.84
SnO_2/PEIE/$Cs_2AgBiBr_6$	0.36	0.40	1.19

4 Methods of analysis

4.1 TRPL analysis

The decay traces are fitted with a stretched-exponential function in the form of [4, 5]:

$$I(\mathrm{t}) = I_0 e^{-(t/\tau)^{\beta}} \quad \textbf{(Eq. S1)}$$

where I(t) is the luminescence intensity changing with time, I_0 is the initial luminescence intensity, τ is the time taken for luminescence intensity to decrease to 1/e of I_0, and β is the distribution coefficient. The formula of average carrier lifetime $<\tau>$ is

$$<\tau>=\frac{\tau}{\beta}\Gamma(\frac{1}{\beta}) \quad \textbf{(Eq. S2)}$$

4.2 SCLC analysis

In the SCLC test, the linear relation of J-V curve in low voltage range is ohmic region. As the voltage continues to increase, the current density rises sharply and the J-V curve deviates from linear relationship, which goes into the trap filling limit (TFL) region. Once all the traps are filled by the carriers, the J-V curve turns into a quadratic relationship, which is trap-free region. The trap filling limit voltage (V_{TFL}) is defined

as the voltage at the intersection of two fitting lines in the ohmic region and the TFL region. The defect density of states of $Cs_2AgBiBr_6$ films can be calculated by the following equation[6]:

$$N_t = \frac{2\varepsilon\varepsilon_0 V_{TFL}}{eL^2} \quad \textbf{(Eq. S3)}$$

where N_t is the defect density, e is the electronic charge, L is the thickness of $Cs_2AgBiBr_6$, V_{TFL} is the limit voltage of defect filling, ε represents the relative permittivity of $Cs_2AgBiBr_6$, ε_0 represents the vacuum permittivity.

The charge mobility (μ) could be calculated from the trap-free region of the SCLC curve using the Mott-Gurney law with the following equation[7]:

$$\mu = \frac{8JL^3}{9\varepsilon_0\varepsilon V^2} \quad \textbf{(Eq. S4)}$$

where μ, J, L, ε_0, ε, and V is the charge mobility, current density, thickness of the $Cs_2AgBiBr_6$ film, vacuum permittivity, relative permittivity of $Cs_2AgBiBr_6$, and voltage, respectively.

4.3 Mott-Schottky analysis

The built-in potential (V_{bi}) can be extracted from the capacitance-voltage measurement with the Mott-Schottky equation[8]:

$$C^2 = \frac{2(V_{bi} - V)}{\varepsilon_0\varepsilon eNA^2} \quad \textbf{(Eq. S5)}$$

where C, V_{bi}, V, ε_0, ε, e, N, and A is the capacitance, built-in potential, applied bias, vacuum permittivity, relative permittivity of $Cs_2AgBiBr_6$, elementary charge, carrier density, and active area of PSC, respectively.

References

1. F. Igbari, R. Wang, Z.-K. Wang, X.-J. Ma, Q. Wang, K.-L. Wang, Y. Zhang, L.-S. Liao and Y. Yang, *Nano Lett.*, 2019, **19**, 2066-2073.
2. P. Pistor, M. Meyns, M. Guc, H.-C. Wang, M. A. L. Marques, X. Alcobé, A. Cabot and V. Izquierdo-Roca, *Scr. Mater.*, 2020, **184**, 24-29.
3. S. J. Zelewski, J. M. Urban, A. Surrente, D. K. Maude, A. Kuc, L. Schade, R. D. Johnson, M. Dollmann, P. K. Nayak, H. J. Snaith, P. Radaelli, R. Kudrawiec, R. J. Nicholas, P. Plochocka and M. Baranowski, *J. Mater. Chem. C*, 2019, **7**, 8350-8356.
4. L. Zhang, B. Han, Z. Liu, Y. Yao, L. Xu, P. Wang, P. Lin, X. Wu, X. Yu and C. Cui, *J. Alloys Compd.*, 2022, **911**, 164972.
5. L. Xu, Y. Qiang, K. Xiao, Y. Zhang, J. Xie, C. Cui, P. Lin, P. Wang, X. Yu, F. Wu and D. Yang, *Appl. Phys. Lett.*, 2017, **110**, 233113.
6. H. Wang, S. Cao, B. Yang, H. Li, M. Wang, X. Hu, K. Sun and Z. Zang, *Sol. RRL.*, 2020, **4**, 1900363.
7. J. Dou, C. Zhu, H. Wang, Y. Han, S. Ma, X. Niu, N. Li, C. Shi, Z. Qiu, H. Zhou, Y. Bai and Q. Chen, *Adv. Mater.*, 2021, **33**, 2102947.
8. J. Qiu, Q. Zhou, D. Jia, Y. Wang, S. Li and X. Zhang, *J. Mater. Chem. A*, 2022, **10**, 1821-1830.